

Dhanvada M. Rao  
Vigyan Research Associates, Inc.  
Hampton, Va., USA

### Abstract

The Upper Vortex Flap (UVF) is a multi-purpose surface concept to improve the subsonic aerodynamics of highly swept delta wings. Hinged along the leading edges and deployed from the wing upper surface, the UVF generates a vortex inboard on the wing in addition to the leading-edge vortex acting on the flap. The relative suction levels on the wing and on the flap surface, governed by the flap angle and angle of attack, lead to a variety of functional applications viz. lift increment, drag modulation, lift/drag improvement and roll augmentation. This paper presents wind tunnel force and pressure measurements on a 74-deg. flat plate delta to define the UVF-related vortex effects and to assess its potential as a versatile control surface in different angle-of-attack regimes.

### List of Symbols

b <sub>F</sub>	Flap span
C <sub>A</sub>	Axial force coefficient
C <sub>D</sub>	Drag coefficient
C <sub>L</sub>	Lift coefficient
C <sub>l</sub>	Rolling moment coefficient
C <sub>m</sub>	Pitching moment coefficient
C <sub>n</sub>	Yawing moment coefficient
C <sub>p</sub>	Static pressure coefficient
C <sub>p,PEAK</sub>	Peak negative pressure coefficient
C <sub>y</sub>	Side force coefficient
L/D	Lift/Drag ratio
α	Angle of Attack
δ <sub>E</sub>	Elevon deflection (differential for positive roll)
δ <sub>F</sub>	Flap deflection (normal to leading edge)
η	Fractional semi-span distance from wing center-line

### I. Introduction

The well-known subsonic limitations of highly swept, slender supersonic-cruise wings have been the focus of considerable research activity in recent years (as exemplified by the papers in ref. 1). Excessive drag, longitudinal instability, and lateral control deficiency have been identified as problems arising from leading-edge separation at higher angles of attack. Although leading-edge camber has been considered for slender wings to obtain attached flow to a specified lift coefficient, the required degree of camber would not be acceptable in supersonic cruise; mechanization of the leading-edge for variable camber may impose intolerable weight penalty as well as loss of internal volume.

Elimination of leading-edge separation unfortunately results in loss of vortex-lift which is a significant component of the total lift on slender wings. Trailing-edge flaps are of limited use on such wings because of the associated large pitching moments. To generate adequate lift at restricted angles of attack for improved field performance of supersonic-cruise aircraft remains a challenge.

An alternative to attached flow for improving the low-speed aerodynamics of highly-swept wings is via controlled three-dimensional separation and vortex management. This radical approach formed the basis of recent NASA-Langley studies of vortex control devices, a notable example being the Vortex Flap. This is a sharp leading-edge flap deflected downwards at an angle less than the up-wash, generating a vortex whose concentrated suction on the flap chord produces a thrust component without complete loss of vortex lift. The vortex flap even in its simplest form demonstrated significant drag-reductions in Langley wind tunnel tests on a variety of basic wing geometries as well as aircraft configuration models (refs. 2-8).

Encouraged by the above results, conceptual variations of the vortex flap were pursued with a view to enhancing the utility of the device. One variation studied was the 'extended' vortex flap for generating a two-vortex system, one on the flap for drag reduction and the other inboard on the wing for lift improvement (ref. 2). It was reasoned that this type of vortex pattern might still be realized with only the upper part of the extended flap present, leading to the configuration of this investigation. This paper combines the results of separate pressure and balance tests, supplemented by flow visualization in an attempt to delineate the basic aerodynamics of the Upper Vortex Flap in a variety of operational modes.

\*This research was supported by NASA Langley Research Center

## II. The Upper Vortex Flap (UVF)

The flap is hinged close to the wing leading edge and when retracted it conforms to the wing upper surface (fig. 1). In operation, the flap is raised (somewhat like a spoiler) to force separation from its free trailing edge. In contrast to the unsteady, turbulent wake generated by the spoiler however, the highly swept trailing edge of UVF and the presence of an adjacent wing surface for flow attachment ensure the formation of a stable, spiral vortex behind the flap. The flow pattern associated with this so-called inboard vortex, depicted in fig. 2A, exists at low angles of attack when the free-stream attachment occurs on the flap surface. The vortex-induced suction on the exposed inboard wing area (i.e. external to the flap overlap) contributes a lift increment.

The Upper Vortex Flap thus produces lift at zero and small angles of attack by forcing vortices that resemble a planar-delta vortex flow at higher angles of attack. Associated with this lift increment will be a drag force mainly due to the vortex suction behind the flap. At higher angles of attack however, when the free-stream attachment moves to the wing lower surface, a leading-edge separation vortex acts on the forward face of the flap to generate a thrust component, as depicted in fig. 2B. The leading-edge vortex continuously expands with increasing angle of attack until the reattachment moves off the flap surface. The two distinct vortex patterns of fig. 2 will lead to changing aerodynamic characteristics. Recognizing the option of asymmetric flap deployment (or deflecting the flap only on one side), a variety of functional applications of the UVF may be envisaged as depicted in fig. 3.

## III. Experimental Details

The basic force model was a flat plate delta with 74 deg. swept, symmetrically-bevelled sharp leading edges. An integral body housed a six-component strain gage balance fixed to a sting support. The major dimensions of the model are indicated in fig. 4.

The Upper Vortex Flaps constructed of aluminum plate were of inverse-taper planform to accommodate the conical expansion of the leading-edge vortex, thus utilizing the flap area more effectively for drag reduction up to higher angles of attack (ref. 2). Three pairs of flaps were built to different sizes as specified by the spanwise width at the trailing edge viz. 2, 4, and 5 inches. The flaps were attached to the wing by means of solid aluminum corner wedges running the full length of the flap, simulating flap deflections of 20-deg., 30-deg., 40-deg., and 50-deg. (measured in a plane normal to the leading edge). The wedges were pointed at the forward end but left blunt at the rear. Asymmetric flap configurations were obtained by removing the right-hand flap and its wedge. The model was tested in the NASA Langley 7 x 10 foot High Speed Tunnel at a nominal Mach number of 0.2 giving a Reynolds number of  $2.0 \times 10^6$  based on the wing mean chord. All aerodynamic coefficients are referred to the

basic wing area.

Supplementary pressure measurements were obtained on a smaller 74-deg. flat plate delta model with Upper Vortex Flaps in the North Carolina State University subsonic wind tunnel. Upper-surface static pressures were measured in a chordwise direction on the flap and spanwise on the wing, at flap deflections between 30-deg. and 70-deg. and angles of attack from 0-deg. to 16-deg. Comparative pressure data were also obtained on a planar delta wing model of identical geometry.

## IV. Discussion of Results

### Flow Visualization

Low-speed smoke visualization trials were performed on the force model with a 30-deg. UVF. Typical photographs of the flow patterns observed in a crossflow plane are presented in fig. 5 for two angles of attack. At low angle of attack ( $\alpha = 5$  deg.) the inboard vortex is clearly visible whereas at  $\alpha = 20$  deg., typical of the high angle of attack case a large, closed region of separation containing a vortex appears above the flap. These slow-exposure photographs attest to the steadiness of the vortex-stabilized separated flows associated with the UVF over a rather wide angle of attack range.

### Pressure Measurements

Restricted to the upper surfaces of wing and flap, these measurements were aimed at obtaining an indication of the suction levels generated by the UVF vortex system in comparison with the planar delta, and of the relative effects of flap angle and angle of attack variations. This background information was hoped to provide a better appreciation of the force results to follow, as well as to guide the efforts towards theoretical modelling of the flow.

UVF deflection effects on the wing pressures are shown in fig. 6. The  $\alpha = 0$  deg. data (typical of the low-alpha range) show a suction peak at the anticipated position of the inboard vortex. The  $-C_{p,PEAK}$  and also the suction level across the central part of the wing are progressively enhanced up to the highest deflection angle ( $\delta_F = 70^\circ$ ). On the other hand, at high angles of attack represented by the data for  $\alpha = 16$  deg., the flap generated suction peaks lie below the planar wing level. The effects of flap angle and angle of attack on the inboard-vortex peak suction are summarized in fig. 7.

Detailed flap chordwise pressure distributions at 2-deg. increments of alpha are presented in fig. 8, separately for the three flap angles. While the pressures at  $\alpha = 0$  deg. are indicative of attached flow, with increasing angle of attack the onset and growth of leading-edge vortex are reflected in a growing suction peak and its gradual movement downstream over the flap chord. A distinctive feature in the 30-deg. UVF data, emerging towards the highest angles of attack is the high suction near the flap trailing edge; it is believed to be associated with a secondary

vortex generated by separation of the entrained flow under an expanded leading-edge vortex which has overgrown the flap chord. At  $\delta_F = 50$  deg. and 70 deg., the absence of this feature indicates that the vortex was contained wholly on the flap to the highest angle of attack. The flap peak suction data are summarized in fig. 9 which offers an instructive comparison with fig. 7. Evidently, suction peaks significantly in excess of the planar wing can be generated at a given angle of attack on the UVF surface just as inboard on the wing. However, whereas high suction peaks on the wing occur at low alpha and with large flap deflections, on the flap surface this happens at higher alpha and relatively small flap angles. Thus is the UVF able to switch its role from a lift-augmentor at low angles of attack to a drag-reducer at high angles of attack.

#### Force Measurements

Symmetric UVF - The effects of flap size and deflection on lift increment versus angle of attack are shown in fig. 10; in general, a positive increment over the planar delta wing is obtained at low angles of attack changing to negative  $\Delta C_L$  at higher alpha. The incremental lift at zero angle of attack shown in fig. 11 for the three flaps, indicates that there is an optimum flap size. The trend of increasing  $\Delta C_L$  with flap deflection at  $\alpha = 0$  deg. is maintained with all flaps up to the highest  $\delta_F (= 50^\circ)$ . Increasing flap angle intensifies the inboard vortex, at the same time exposing more of the wing area; accordingly the lift increment is expected to continue with further flap deflection (see pressure results).

Considering only the results for the 4-inch flap (i.e. one closest to optimum size) for further discussion, the incremental drag results are presented in fig. 12. The drag increase at lower angles of attack changes to drag-reduction at higher alpha, following the change-over from the initially inboard-vortex dominated flow pattern to one dominated by the leading-edge vortex. The wedges adopted for convenience of flap installation on the model obviously were not representative of full-scale practice, thereby resulting in unrealistic installation drag; nevertheless, the data trends with flap deflection angle as well as with angle of attack are expected to be valid.

The lift and drag increments due to UVF deployment produce a substantial improvement in lift/drag ratio at higher angles of attack, as shown in fig. 13. This L/D improvement, in spite of the negative lift increment at these angles of attack, implies significant thrust effectiveness of the Upper Vortex Flaps. On the other hand, at low angles of attack when the leading-edge vortex is absent, the UVF generates substantial drag typified by the zero-alpha  $\Delta C_D$  presented in fig. 14. The drag-increment is almost proportional to the flap size, as should be expected. The linearity of drag increase with flap deflection together with the steady nature of the vortex-associated flow suggests the use of UVF as a drag modulator and for rapid deceleration both in flight and on the runway.

The pitching-moment characteristics are shown in fig. 15. The moment reference point was selected to yield a slightly positive static stability of the planar wing at low angles of attack. The planar wing data show a pitch-up at  $\alpha = 8$  deg. approx.; the UVF virtually eliminates this longitudinal instability. A small positive pitching moment produced at the highest flap angle can be trimmed out by a positive trailing-edge flap deflection which will add to lift. The absence of large pitch variation with UVF deployment is an additional advantage in using it for aerodynamic braking.

Non-Symmetric UVF - With the UVF deflected only on one leading edge, aerodynamic characteristics are obtained which have potential for lateral-directional control applications; furthermore the variation of these forces and moments with angle of attack serves as an indicator of the changing relative strength of the associated vortices. The incremental force and moment coefficients (relative to the planar wing) due to a flap deflection of 50 deg. shown in fig. 16 are typical. As already noted in the symmetric UVF results, the normal-force and axial-force increments change from positive to negative with increasing alpha. This reflects the changing balance between the suction induced by the inboard vortex behind the flap and on the wing, and that induced by the leading-edge vortex on the forward face of the flap, as was illustrated by the pressure data previously discussed. The variations with angle of attack of lateral/directional coefficients provide further evidence in this regard: a positive side force generated at low alpha by the left-hand UVF becomes negative at  $\alpha > 13$  deg. following the axial force trend; the yawing moment concurrently changes sign but in reverse direction, indicating that the side force acts aft of the c.g. (i.e. in the vicinity of the flap area center). The rolling moment generally remains small until reaching  $\alpha = 13$  deg. when it assumes a strong positive trend, which can be explained by the onset of a concentrated suction due to the leading-edge vortex on the flap surface, while the plain leading-edge vortex on the opposite wing panel is moving inboard, resulting in a lateral C.P. movement towards the left-hand panel. It is noteworthy that this positive rolling-moment trend is accompanied by a positive viz. a favorable yawing moment.

The potential of asymmetric UVF deflection for roll-power improvement at high angles of attack is of particular interest because of lateral control limitations generally encountered on highly-swept delta wings. Rolling-moment data for the 4-inch flap at various deflection angles are presented in fig. 17. The indicated trends with angle of attack and flap deflection suggested that an asymmetric UVF configuration might be used to augment the effectiveness of conventional elevons at high alpha. Additional data were obtained with a pair of elevons added to the wing trailing edge and with a 20 deg. UVF on the left-hand leading edge. Rolling moments with 0 deg.,  $\pm 10$  deg. and  $\pm 20$  deg. of elevon deflection for positive roll, are presented in fig. 18. In retrospect, a better choice would have been the 30-deg. UVF which sustains the roll

increment to higher angles of attack than does the 20-deg. UVF (see fig. 17); the present results are thus conservative. A substantial augmentation of the elevon rolling power in the presence of asymmetric UVF is seen, starting from  $\alpha = 10$  deg. The nature of this augmentation suggests that the UVF/elevon is a synergistic combination i.e. the combined roll power exceeds the sum of the individual contributions (compare the shaded regions with and without elevon deflection, fig. 18). This result is believed to be due to additional suction induced by the inboard vortex over the down-elevon. The same augmentation mechanism would also be expected to improve trailing-edge flap effectiveness in combination with symmetric UVF for better lift-increment capability.

Two indirect aerodynamic effects of roll-control deflection need to be considered: a yawing moment which if adverse will degrade handling in tight turns, and a drag increment which will reduce sustained-turn performance. The roll-associated yawing moment shown in fig. 19 is seen to be proverse at the angles of attack when UVF provides positive roll-augmentation. The effect of incremental drag due to roll controls is presented in terms of lift/drag ratio in fig. 20, which points to a further benefit of using UVF in combination with elevons. Evidently, the thrust effect of the single UVF was sufficient to cancel out the drag increase due to 10 deg. of elevon while augmenting the roll power by nearly 33%, in the  $C_L$  range 0.4 to 0.8. A more optimum UVF deflection than 20 deg. employed in these tests should yield even better performance.

#### V. Computational Results

As part of a NASA- Langley effort towards assessment of the capabilities of the Boeing Free Vortex Sheet method (ref. 9), a few attempts were made to model the Upper Vortex Flap. A 74-deg. planar delta with a full-span 'conical' flap was successfully computed with separation fixed at the flap trailing edge; however, limited attempts at simulating a two-vortex flow (i.e. including leading-edge separation) failed to converge.

The computed aerodynamic coefficients for a particular flap deflections are compared with the present balance data in fig. 21. Good agreement is found except towards higher angles of attack when the leading-edge vortex, not modelled in the computation, begins to dominate. The calculated spanwise pressure distributions sampled at 5 deg. and 20 deg. angles of attack (fig. 22) are representative of the inboard-vortex flow field; although direct comparison with the present pressure data is not warranted in view of the differences in the flap geometry, the calculated magnitude and spanwise location of the suction peaks are in the right order. Further trials are needed to more completely evaluate the FVS method for UVF configurations with two-vortex representation.

#### VI. Concluding Remarks

The Upper Vortex Flap Concept has been evaluated as a multi-purpose aerodynamic surface for improved subsonic performance and control of highly

swept delta wing configurations. Exploratory wind tunnel tests on a 74-deg. flat plate delta model showed that the UVF:

- 1) Established a stable two-vortex pattern, the relative strengths of the inboard and leading-edge vortices varying with angle of attack and flap angle,
- 2) Produced a lift increment (over the planar delta) at zero and low angles of attack, useful for slow approach and landing with improved forward view,
- 3) Generated drag increments with a steady separated flow-field, useful for rapid deceleration in flight and on runway,
- 4) Improved longitudinal stability by eliminating pitch-up,
- 5) Improved lift/drag ratio in the  $C_L$  range 0.4 to 0.6, offering increased efficiency during climb and loiter, and
- 6) Augmented roll control at high angles of attack when used asymmetrically in combination with elevons, with favorable yaw and drag characteristics for improved handling and performance in turns.

The above capabilities appear inherent to the UVF concept, being consistent with the associated vortex aerodynamics. The level of flap effectiveness can be potentially improved over the present results through refinements of the flap geometry in order to enhance the vortex strength and persistence characteristics.

#### References

1. Supersonic Cruise Research 1979, NASA Conference Publication 2108.
2. "Leading Edge Vortex Flap Experiments on a 74-Deg. Delta Wing", Rao, D. M., NASA CR 159161, (1979).
3. "Exploratory Subsonic Investigation of Vortex Flap Concept on Arrow Wing Configuration", Rao, D. M., NASA CP 2109 (Part I), pp. 117-129, (1979).
4. "Leading Edge Vortex Flaps for Enhanced Subsonic Aerodynamics of Slender Wings", Rao, D. M., 12th Congress of the International Council of the Aeronautical Sciences of Munich, Proceedings. pp. 554-562, 1980.
5. "Design Related Study of Transonic Maneuvering Slender Wings Having Vortex Flow", Lamar, J. E. and Campbell, J. F., Tactical Aircraft Research and Technology Conference, NASA CP 2162, Part 2, Vol. I., pp. 543-562, 1980.
6. "Experimental Results of a Leading-Edge Vortex Flap on a Highly Swept Cranked Wing", Smith, W.; Campbell, J. F.; and Huffman, J. K., Tactical Aircraft Research and Technology Conference, NASA CP 2162, Part 2, Vol. I, pp. 563-580, 1980.

7. "Wind Tunnel Investigation of Vortex Flaps on a Highly-Swept Interceptor Configuration", Schoonover, W. E., Jr. and Ohlson, W. E., Paper ICAS-82-6.7.3. 13th Congress of the International Council of the Aeronautical Sciences, Seattle, 1982.
8. "Analytical Study of Vortex Flaps on Highly Swept Delta Wings", Frink, N. T., Paper ICAS-82-6.7.2. 13th Congress of the International Council of the Aeronautical Sciences, Seattle, 1982.
9. "Aerodynamic Performance of Slender Wings with Separated Flows", Reddy, C. S. O.D.U. Research Foundation Tech. Rep., March 1982.

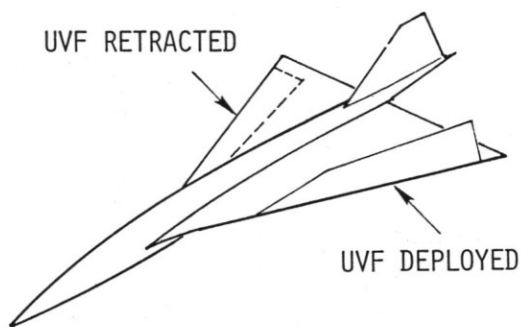


Fig. 1 - Upper Vortex Flap (UVF) Concept

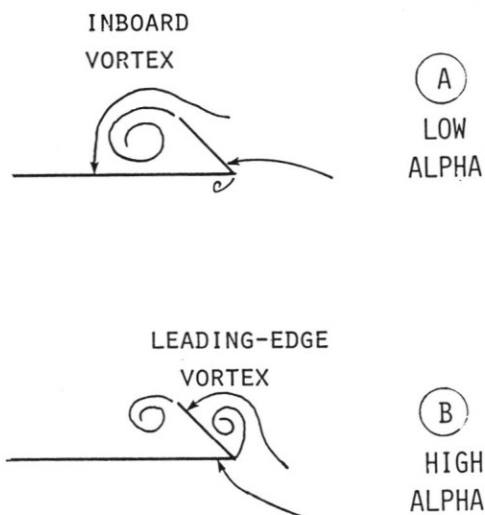


Fig. 2 - Vortex patterns associated with UVF (viewed in a plane normal to the leading edge)

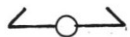
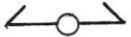
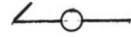
			
UVF CONFIG. →	SYMMETRIC	SYMMETRIC	ASYMMETRIC
$\alpha$ RANGE →	ZERO & LOW ALPHA	MODERATE ALPHA	MODERATE & HIGH ALPHA
UVF FUNCTION →	AUGMENT LIFT ; MODULATE DRAG	AUGMENT L/D	AUGMENT ROLL POWER
FLIGHT REGIME →	LANDING ; GROUND ROLL	CLIMB ; LOITER ; APPROACH	MANEUVER ; CROSS-WIND APPROACH

Fig. 3 - Conceptual applications of the UVF

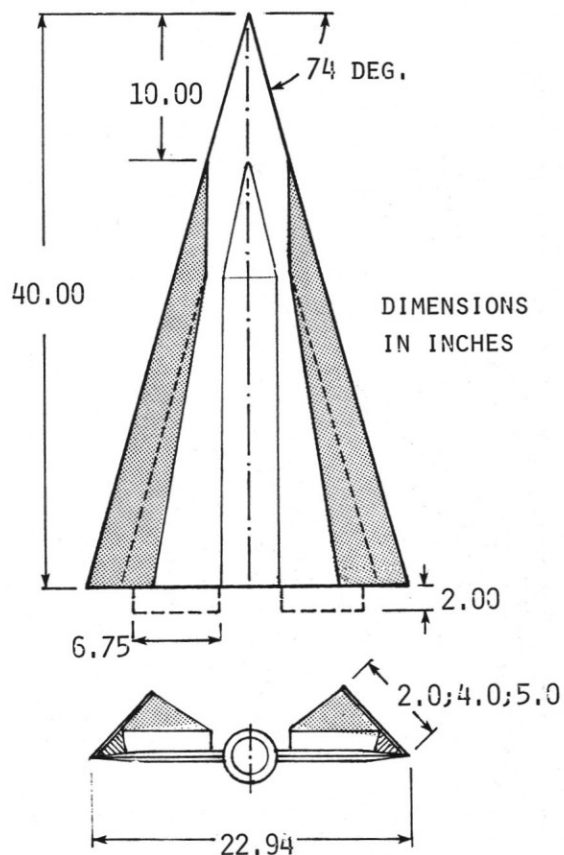


Fig. 4 - Details of UVF force model

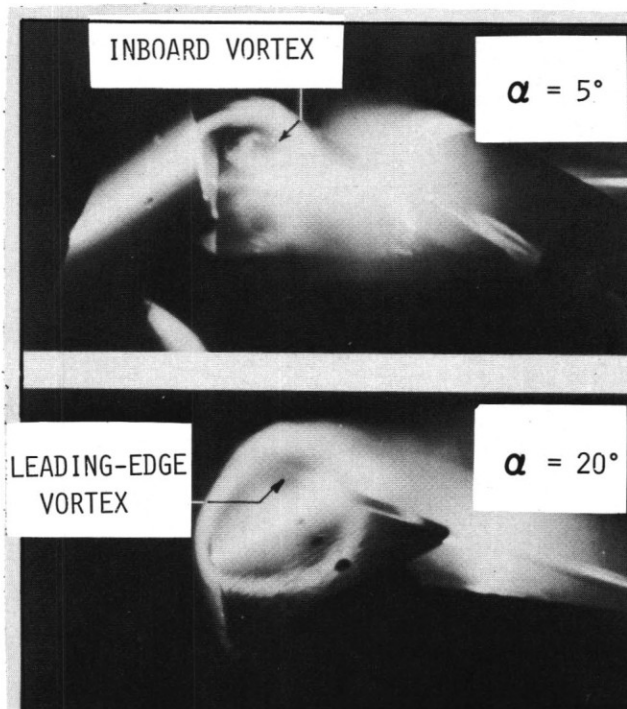


Fig. 5 - Smoke visualization of UVF vortex patterns

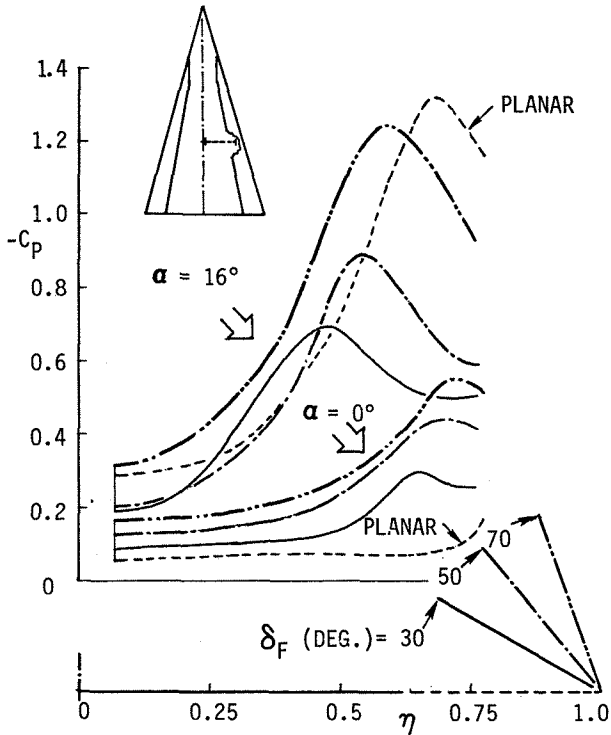


Fig. 6 - Typical spanwise pressure distributions on wing with UVF

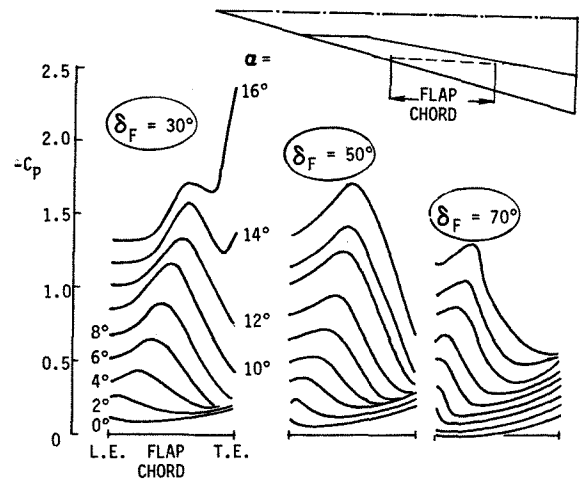


Fig. 8 - UVF chordwise pressure distributions

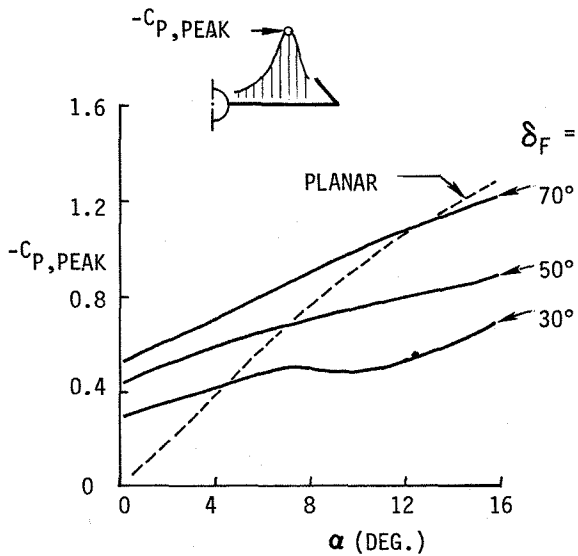


Fig. 7 - Development of inboard suction peak on the wing with UVF

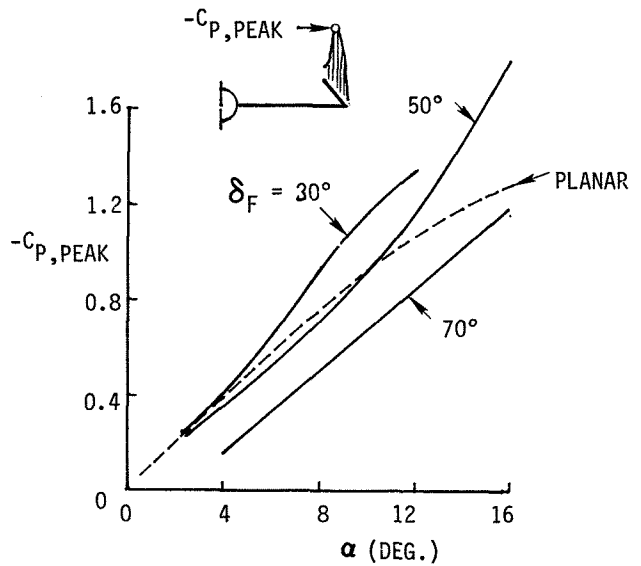


Fig. 9 - Development of UVF suction peak

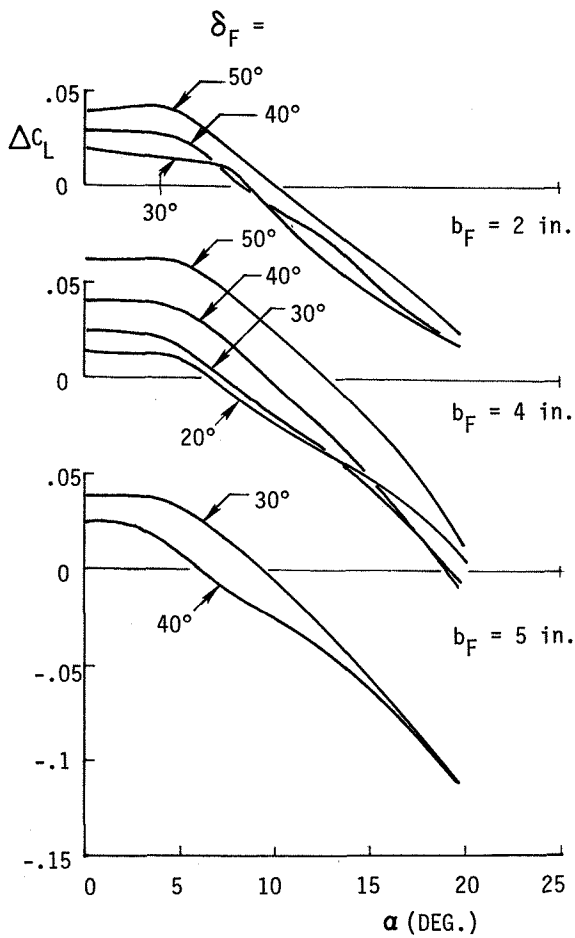


Fig. 10 - Lift increment due to UVF

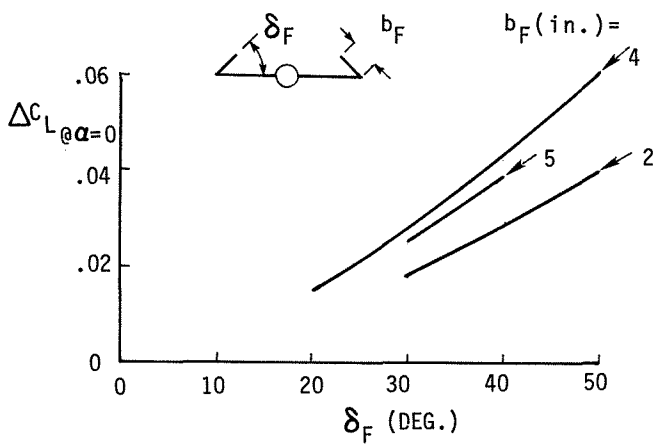


Fig. 11 - UVF lift increment at zero angle of attack

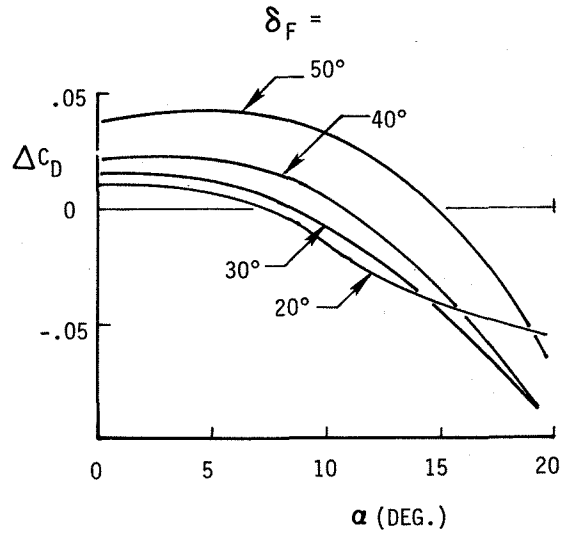


Fig. 12 - Drag increment due to UVF

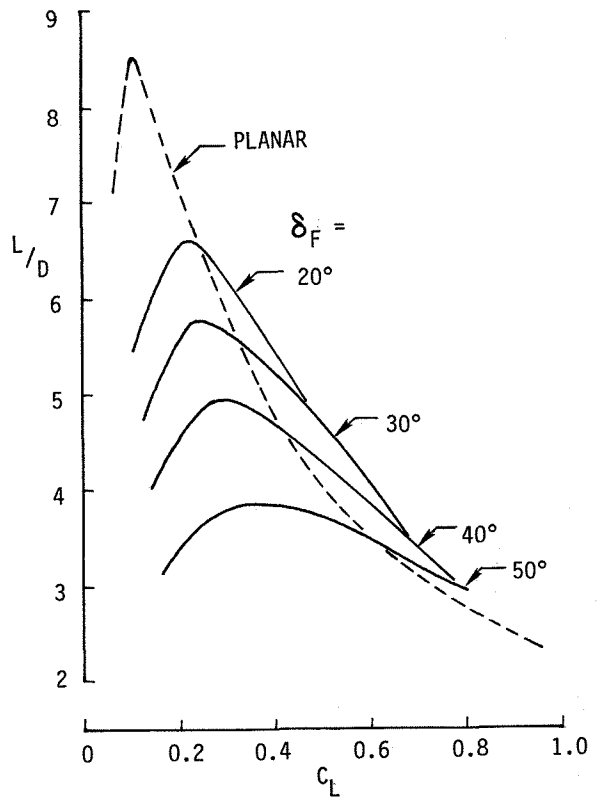


Fig. 13 - Lift/Drage ratio improvement due to UVF



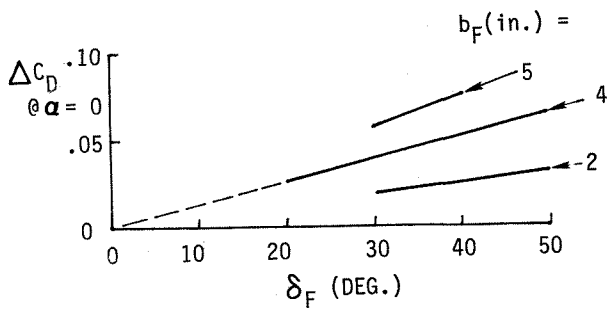


Fig. 14 - UVF drag increment at zero angle of attack

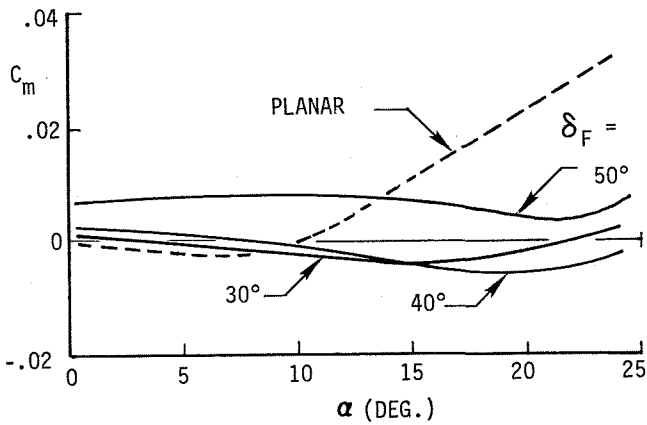


Fig. 15 - Pitching moment characteristics with UVF

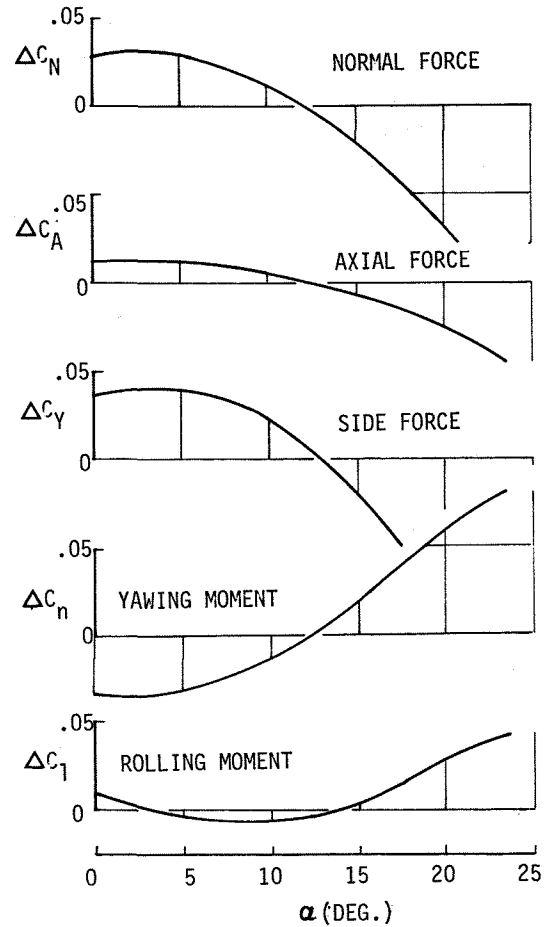


Fig. 16 - Incremental aerodynamic coefficients with asymmetric UVF

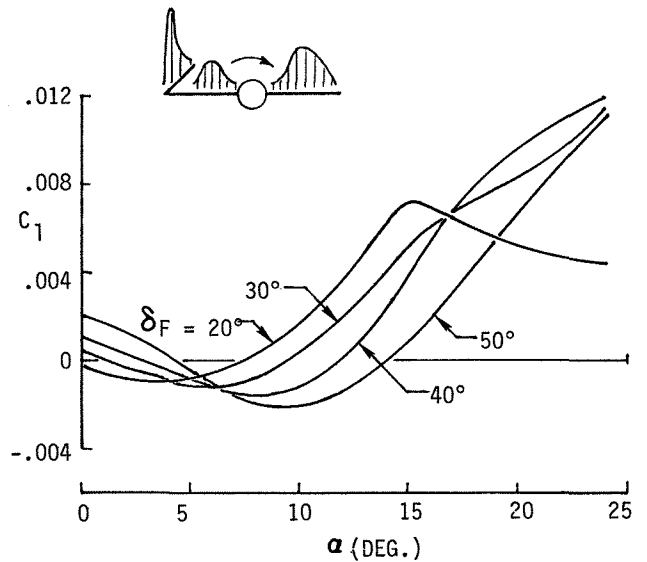


Fig. 17 - Rolling moment with asymmetric UVF

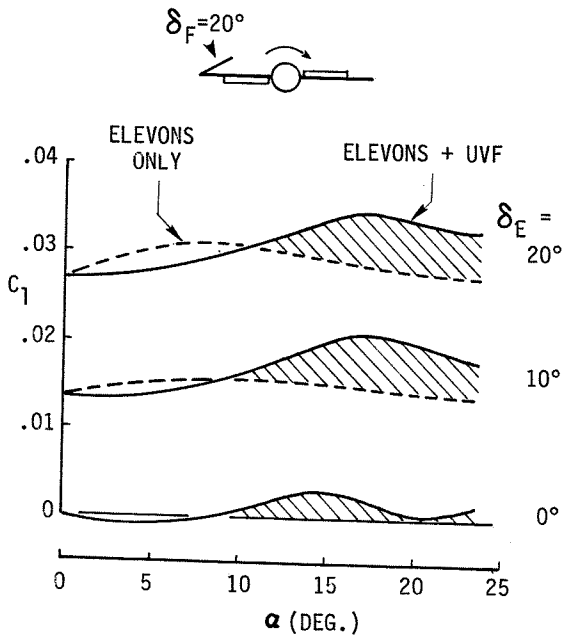


Fig. 18 - Rolling moment with UVF/elevon combination

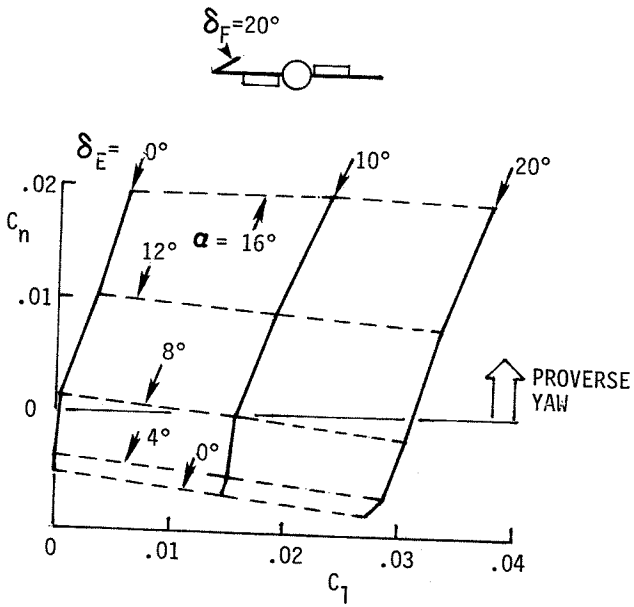


Fig. 19 - Roll-associated yawing moment with UVF/elevon combination

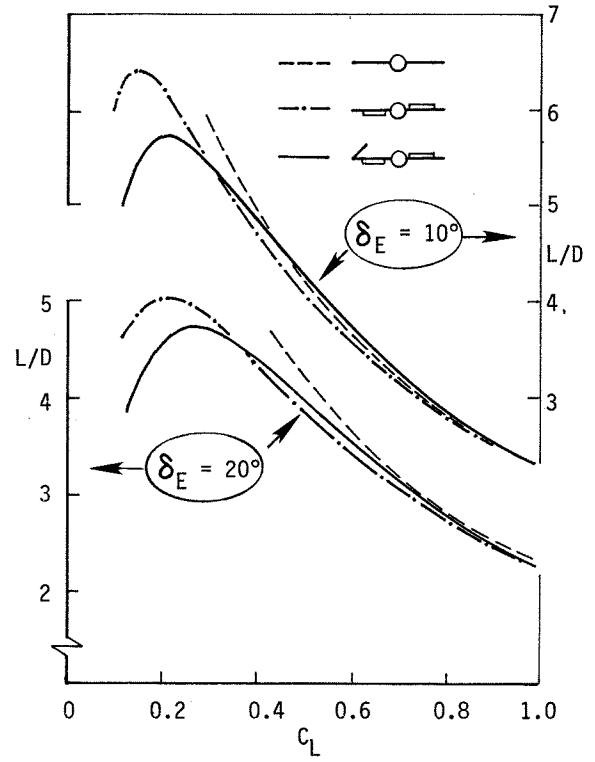


Fig. 20 - Lift/Drag ratio with roll controls

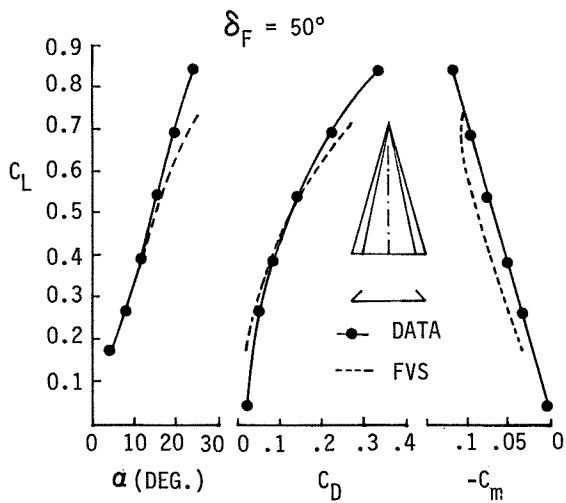


Fig. 21 - Free Vortex Sheet computation of UVF aerodynamic coefficients versus experiment

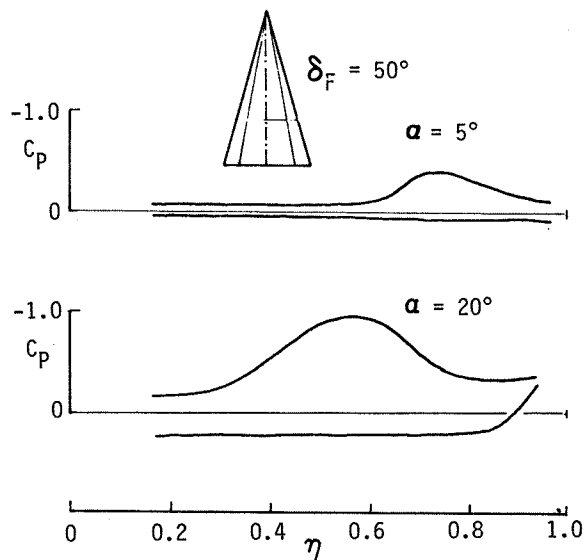


Fig. 22 - Computed wing spanwise pressure distributions by Free Vortex Sheet method